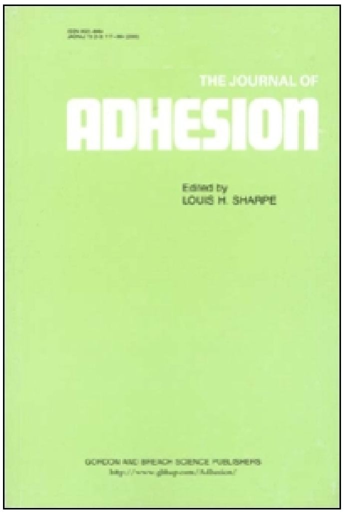

The Journal of Adhesion
Publication details, including instructions for authors and subscription information:
http://www.informaworld.com/smpp/title~content=t713453635

WETTABILITY AND SURFACE ENERGETICS OF ROUGH FLUOROPOLYMER SURFACES

R. Sedev[a]; M. Fabretto[a]; J. Ralston[a]
[a] Ian Wark Research Institute, University of South Australia, Mawson Lakes, Australia

To cite this Article Sedev, R. , Fabretto, M. and Ralston, J.(2004) 'WETTABILITY AND SURFACE ENERGETICS OF ROUGH FLUOROPOLYMER SURFACES', The Journal of Adhesion, 80: 6, 497 — 520
To link to this Article: DOI: 10.1080/00218460490477161
URL: http://dx.doi.org/10.1080/00218460490477161

The Journal of Adhesion, 80: 497–520, 2004

ISSN: 0021-8464 print/1545-5823 online
DOI: 10.1080/00218460490477161

WETTABILITY AND SURFACE ENERGETICS OF ROUGH FLUOROPOLYMER SURFACES

R. Sedev
M. Fabretto
J. Ralston
Ian Wark Research Institute, University of South Australia,
Mawson Lakes, Australia

Hydrophobic solid surfaces with controlled roughness were prepared by coating glass slides with an amorphous fluoropolymer (Teflon® AF1600, DuPont) containing varying amounts of silica spheres (diameter 48 μm). Quasi-static advancing, θ_A, and receding, θ_R, contact angles were measured with the Wilhelmy technique. The contact angle hysteresis was significant but could be eliminated by subjecting the system to acoustic vibrations. Surface roughness affects all contact angles, but only the vibrated ones, θ_V, agree with the Wenzel equation. The contact angle obtained by averaging the cosines of θ_A and θ_R is a good approximation for θ_V, provided that roughness is not too large or the angles too small. Zisman's approach was employed to obtain the critical surface tension of wetting (CST) of the solid surfaces. The CST increases with roughness in accordance with Wenzel equation. Advancing, receding, and vibrated angles yield different results. The θ_A is known to be characteristic of the main hydrophobic component (the fluoropolymer). The θ_V is a better representation of the average wettability of the surface (including the presence of defects).

Keywords: Contact angle; Surface roughness; Wenzel equation; Average wettability; Acoustic vibrations; Teflon AF1600

Received 26 November 2003; in final form 29 March 2004.

Financial support for this project from the Australian Research Council Special Research Centre Scheme is gratefully acknowledged.

One of collection of papers honoring A. W. Neumann, the recipient in February 2004 of *The Adhesion Society Award for Excellence in Adhesion Science, Sponsored by 3M*.

Address correspondence to Rossen Sedev, Ian Wark Research Institute, University of South Australia, Mawson Lakes, SA 5095, Australia. E-mail: rossen.sedev@unisa.edu.au

INTRODUCTION

The wettability of solid surfaces is of crucial importance in many natural and industrial processes as it significantly affects all ensuing events after contact between the solid and the liquid is made. Wettability will strongly influence the capillary effects in the system and is inherently related to spreading and adhesion [1–6]. From a thermodynamic point of view the wettability is best quantified by the contact angle, θ, formed between the solid–liquid and liquid–vapour interfaces. The Young equation relates the equilibrium contact angle to the interfacial tensions of the three interfaces intersecting each other at the contact line [1]:

$$\cos\theta = \frac{\gamma_S - \gamma_{SL}}{\gamma}. \tag{1}$$

In the above equation γ_S, γ_{SL}, and γ denote the interfacial tensions of the solid–vapour, solid–liquid, and liquid–vapour interfaces, respectively. The Young equation has been extensively discussed over the years and provides a solid thermodynamic foundation for understanding the wetting properties of an equilibrium three-phase system. It refers, however, to a rather ideal solid surface—one that is effectively inert, flat, smooth, and of homogeneous composition. One important feature of the Young equation is that it could be used to quantify the surface tension of the solid, γ_S. The possibility is made all the more appealing since contact angle measurements are rather simple and relatively inexpensive. However, the solid surface tension of solids cannot be measured and, therefore, the term τ_S ($= \gamma_S - \gamma_{SL}$, known as "adhesion tension," "wetting tension," or "work of immersional wetting per unit area") cannot be resolved into components; therefore, an additional relation is required to solve the problem.

Zisman [1, 5] has developed an empirical approach, which consists of examining the contact angles of various liquids on one and the same solid surface. The results are often well described by the linear relation

$$\cos\theta = 1 - \alpha(\gamma - \gamma_C). \tag{2}$$

The critical surface tension of wetting of the solid, γ_C, is related to the surface tension of the solid. The slope, α, is usually assumed to be constant ($0.03–0.04\,\mathrm{m^2/mJ}$ [1]) and is rarely discussed. Zisman has explored the fundamental relation between surface composition and wettability in significant detail, and his celebrated review [5] is still a basic reference in the field.

There are several contact angle theories, but unlike the Young equation their validity is often debated. This is hardly surprising since these are, by necessity, attempts to capture the complex interplay of interfacial forces in a three-phase system within a tractable model. We consider only two of the most elaborated theories (typically seen as irreconcilable).

According to Neumann and Spelt [3] the relation $\gamma_{SL} = f(\gamma_S, \gamma)$ exists for thermodynamic reasons and can be formulated in alternative analytical expressions. Perhaps the most compact version of the resulting contact angle Equation is [7]

$$\cos\theta = -1 + 2\mathrm{e}^{-\beta(\gamma_S-\gamma)^2}\left(\frac{\gamma_S}{\gamma}\right)^{1/2}. \tag{3}$$

The proponents of Equation (3) claim that the parameter β is a universal constant, but the conclusion is based on experimental evidence rather than theoretical analysis.

In a radically different approach, the surface tension of the solid–liquid interface (or any other interface for that matter) is split into components [8]. van Oss, Good, and Chaudhury [4, 9–11] have argued that the most appropriate choice of component is

$$\gamma_i = \gamma_i^{LW} + \gamma_i^{AB}. \tag{4}$$

Where the Lifshitz-van der Waals (LW) component lumps together van der Waals-London (dispersive), the Keesom and Debye type of interactions and the Acid-Base (AB) component include the contribution of Lewis acid–base interactions across the interface. Teflon-like surfaces are apolar, *i.e.*, do not possess (because of their chemical nature) the complementary ability to participate in AB interactions with any liquid and, therefore, ${\gamma_S}^{LW} \equiv \gamma_S$. In this case the van Oss-Good-Chaudhury contact angle equation is written as

$$\cos\theta = -1 + 2\frac{\left(\gamma_S\gamma^{LW}\right)^{1/2}}{\gamma}. \tag{5}$$

If only alkanes are used ($\gamma^{LW} \equiv \gamma$ for any alkane), then Equation (5) is reduced to the well-known Girifalco-Good equation [1],

$$\cos\theta = -1 + 2\left(\frac{\gamma_S}{\gamma}\right)^{1/2}. \tag{6}$$

By definition the critical surface tension of wetting is obtained when $\gamma \to \gamma_S$ and $\theta \to 0$. When $\gamma - \gamma_S$ is positive but small Equation (6) can be expanded as [12]

$$\cos\theta = 1 - \frac{1}{\gamma_S}(\gamma - \gamma_S) + O[(\gamma - \gamma_S)^2], \tag{7}$$

the series expansion resembles Zisman's Equation (2) and shows that $\gamma_C = \gamma_S$ (as long as alkanes are used) and $\alpha = 1/\gamma_S$ [12].

Everyday laboratory practice provides many examples surface roughness alters the contact angle (*e.g.*, using a roughened Wilhelmy plate to measure the surface tension of liquids or the spreading pressure of insoluble monolayers, roughen the opposite surfaces before applying the adhesive, etc.). For an ideal solid surface (*i.e.*, as in the Young equation except for the smoothness), the influence of roughness is given by Wenzel's equation [1]:

$$\cos\tilde{\theta} = \frac{A}{A_0}\cos\theta = r\cos\theta. \tag{8}$$

In this equation, $\tilde{\theta}$ is the contact angle measured on the rough surface and r is the ratio of the actual, A, to the projected, A_0, solid surface area. Wenzel's ratio r simply reflects the fact that there is more geometric solid area per nominal unit area [13]. A simplified derivation of Equation (8) can be carried out as follows. If a smooth solid surface is heterogeneous, *e.g.*, consists of patches 1 and 2 (Figure 1a), then the contact angle measured on such a surface should reflect the wettability of both components 1 and 2.

It is given by the Cassie equation [1],

$$\cos\theta_C = \frac{A_1}{A_0}\cos\theta_1 + \frac{A_2}{A_0}\cos\theta_2, \tag{9}$$

where $A_{1,2}$ is the total area of the surface of type 1,2 and A_0 is the total nominal area. Consider a rough surface to be composed of various patches having the same wettability (Figure 1b). The average contact angle, θ_{avg}, on such a surface is

$$\cos\theta_{avg} = \frac{A_1}{A_0}\cos\theta_0 + \frac{A_2}{A_0}\cos\theta_0 + \frac{A_3}{A_0}\cos\theta_0 = \frac{A_1 + A_2 + A_3}{A_0}\cos\theta_0. \tag{10}$$

Since $(A_1 + A_2 + A_3)/A_0 \equiv r$, it follows that Equation (10) is identical to Wenzel's Equation (8). Since $r \geq 1$, according to Equation (8), increasing the roughness should increase obtuse contact angles and reduce acute contact angles. This is a rather frequent experimental observation, though the precise dependence has rarely been quantified.

Rigorous thermodynamic arguments have been used to explore Young and Wenzel equations [13, 14], and therefore questioning their validity would be inappropriate. However, the question of how reliably Equations (1) and (8) can be used to interpret contact angles on real surfaces—where contact angle hysteresis is unavoidable—is a difficult

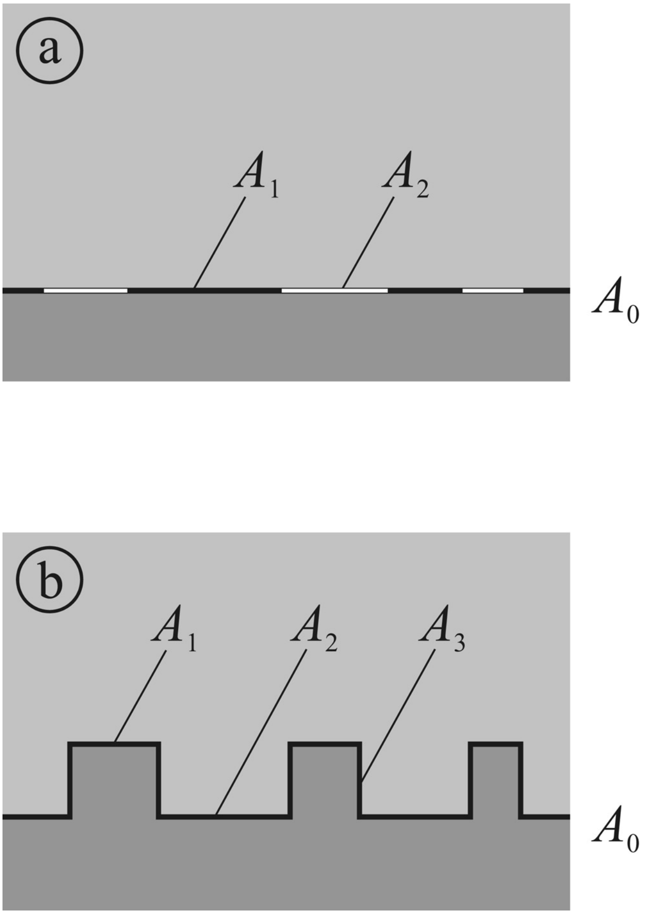

FIGURE 1 (a) Wetting of a smooth, chemically heterogeneous surface. The area of patches type 1 is A_1 and the area of patches type 2 is A_2. The nominal area is A_0. (b) Wetting of a rough, chemically homogenous surface. The area of the elevated patches is A_1. The area of the base patches is A_2. The area of side patches is A_3. The nominal area is A_0.

one and rarely explored. Hysteresis is a problem in its own right. In practically any real system a whole range of contact angles can be achieved, even though the contact line remains static. The advancing, θ_A, and receding, θ_R, contact angles are the upper and lower limits of this interval and most often reported in experiments. Contact angle hysteresis is usually seen as an irreversible phenomenon [6, 10, 13] and is attributed to imperfections—physical and/or chemical—of the solid surface (assuming it is totally inert with respect to the liquid). The influence of roughness, in particular, has a dual effect. On one side, it intrinsically changes the wettability of the surface (as prescribed by Wenzel's equation) but on the other side it also increases the hysteresis, thus making the use of Wenzel equation even less justifiable. The relation between experimentally measured contact angles and the simple Equations (1) and (8) is more complex than is often acknowledged.

Contact angle measurement is a fast, rather simple, relatively inexpensive, and extremely surface-sensitive test. It is widely used, *e.g.*, in materials science. In practice, however, a detailed study of the hysteresis is often beyond the scope of the study and the experimentalist is left with the ambiguous choice of which contact angle (advancing, receding, averaged, etc.) to use in conjunction with Wenzel equation (or equations for that matter). It is our impression that more often than not the choice is guided by local tradition rather than a conceptual perception. Time and again the discussion of the wetting properties of a given surface is decoupled from the elucidation of the hysteresis whose influence is unavoidable. Surface roughness is a prime example of this lack of completeness.

Even for "smooth" solids there are different opinions as to which angle is more representative of the surface. The "Cassie" argument can be used to obtain an average contact angle on a surface with a significant hysteresis. Due to the intrinsic difference between advancing and receding contact angles it can be argued that one and the same physical surface (of nominal area A_0) is probed in two different ways (Figure 2).

Therefore, the average wettability can be expressed as

$$\cos\theta_{avg} = \frac{A_0}{A_0 + A_0}\cos\theta_A + \frac{A_0}{A_0 + A_0}\cos\theta_R = \frac{1}{2}(\cos\theta_A + \cos\theta_R). \qquad (11)$$

Equation (11) was proposed firstly by Adam and Jessop [15].

There is disagreement on how to treat contact angles measured on rough solid surfaces. The situation is probably best illustrated by the two extreme positions: (1) a rather strong rejection of the possibility to understand contact angles on rough surfaces—"all contact angles on rough surfaces are meaningless in terms of the Young equation" [16]; and (2) a mechanistic assumption that consistency can be simply achieved, provided only one type of angle is used, *e.g.*, both advancing and receding contact angles are in conjunction with the van Oss-Chaudhury-Good theory of contact angles and are regarded as totally unrelated [17].

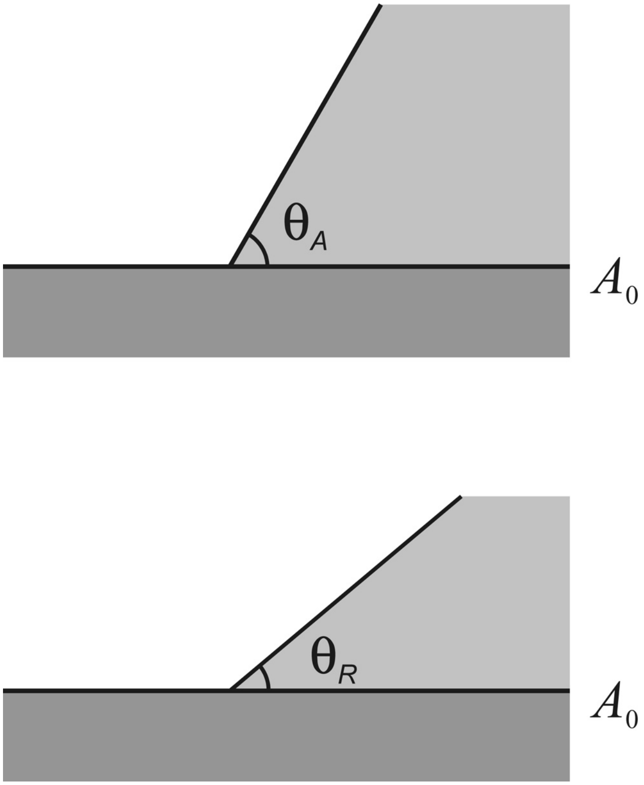

FIGURE 2 Contact angle hysteresis on a real surface of nominal area A_0. The area A_0 is probed twice: during advancing (top) and during receding (bottom).

There have been few articles quantitatively dealing with the influence of roughness *per se*. One reason is that rough surfaces do not have an immediate advantage over smooth ones (*e.g.*, if compared with surfaces patterned with different chemical entities having potentially wide applications). It should be pointed out, however, that, strictly speaking, smooth surfaces do not exist. The fundamental question of at what level does roughness affect the wetting properties has not been answered definitively. Neumann *et al.* [18] concluded that roughness smaller than approximately 0.1 µm has no influence on contact angles. On the other hand, Mason and coworkers found that rugosities of size 50 nm or even less can have an impact on spreading [19]. Therefore, the topic should be explored further.

In this article we investigate the wettability of a hydrophobic (perfluorinated) surface, which was made artificially rough by embedding particles into the polymer coating. We used the Wilhelmy technique to determine quasi-static advancing and receding contact angles. In addition, we have employed external (acoustic) vibrations as a tool for reducing hysteresis. We found that vibrated contact angles follow Wenzel's equation rather closely, *i.e.*, they appear to be a good approximation for the equilibrium contact angles. The contact angle obtained by averaging the cosines of the advancing and receding angles turned out to be a good approximation for the vibrated one, provided that surface roughness is not very large or the angles too small. Finally, a discussion of the surface energetics of rough surfaces is attempted.

MATERIALS AND METHODS

Glass microscope slides ($22 \times 50 \times 0.15\,\mathrm{mm}^3$, Deckglasser, Menzel-Gläser, Germany) were used as substrates. Coarse contamination was removed by sonicating the slides (Soniclean Model 160HT, Soniclean Pty Ltd, Adelaide, SA, Australia) in warm ethanol (Aldrich, spectrophotometric grade) for about an hour. The slides were then removed and abundantly rinsed with pure water (resistivity $\geq 18\,\mathrm{M\Omega{\cdot}cm}$; UHQPS, Elgastat, Elgastat water UK, Bucks, UK). The wet slides were immediately transferred to a plasma cleaner (Harrick Model PDC-32G, Harrick Scientific, Ossining, NY, USA) and treated on medium power setting for 5 min.

Without delay the clean slides were coated with an amorphous fluoropolymer (Teflon AF1600, DuPont (Australia) Ltd, Sydney, NSW, Australia) layer. A 1.5% by weight solution of AF1600 in a perfluorinated solvent (Fluorinert FC-75, 3 M Australia, Pymble, NSW, Australia) was used to dip-coat the slides at a fixed withdrawal speed (10 mm/s). Surfaces with different roughness were produced by adding varying amounts of silica spheres (mean diameter 48 μm, GelTech, Alachua, FL, USA) into the coating mixture. The RMS roughness of the uncoated slides was about 5 nm and is negligible in comparison with the particle-induced roughness. The AF1600 coating was then heat-treated (7 min at 112°C, 5 min at 165°C, and 15 min at 330°C [20]) in order to remove any residual solvent and also to increase the bond strength to the substrate.

The number of particles per unit area, $n\ (= N/A_0)$, was determined from SEM images and the Wenzel ratio was calculated by taking into account the additional geometric area per particle. The results are listed in Table 1, whilst full details can be found in Fabretto *et al.* [21].

A series of probe liquids was used to assess the wettability of the coated surfaces: Octane, Hexadecane, Formamide, and Methylnaphthalene (Sigma-Aldrich Pty Ltd, Sydney, NSW, Australia), Ethylene

TABLE 1 Number of Particles per Unit Area, n, Surface Coverage, ϕ, and Roughness Ratio, r, for All Samples

Sample	$n = N/A_0$ [1/mm^2]	ϕ [%]	r
0*	0.0	0.0	1.00
1	4.4	0.5	1.02
2	8.0	1.0	1.03
3	44.3	5.4	1.16
4	93.7	11.5	1.35

*Smooth, *i.e.*, coated with AF1600 only (without any particles).

glycol and Dimethylformamide (Sigma), Heptane and Dimethyl sulfoxide (BHD Chemicals Merek, Pty Ltd, Kilsyth, UIC, Australia), Hexane (EM Science, Gibbstown, NJ, USA), and water. All liquids were used as received. Their surface tensions were determined by the drop weight method and were comparable with reference values.

Contact angles were determined by the Wilhelmy plate method. Details of the specific setup have been given elsewhere [22–24]. Additionally, an audio speaker was mounted on the driving platform and used to create acoustic vibration on the surface of the test liquid as described in Fabretto *et al.* [21]. The samples were suspended from the balance *via* a thin wire with a polyethylene clasp. The sensitivity of the balance was 1 μN. Advancing and receding contact angles were measured at a constant rate of 50 μm/s. It was independently checked that the values obtained were not significantly affected by liquid motion, *i.e.*, all reported angles are quasi-static. At selected depth of immersion the plate was stopped, acoustic vibration was applied for 70 s, and 10 s later a reading of the force was taken. The barriers preventing the contact line from achieving its equilibrium position (and thus responsible for the contact angle hysteresis) are effectively surmounted when external energy is temporarily supplied to the system (see Fabretto *et al.* [21] for details).

All experiments were carried out in a dust-free environment (Clean Room) at ambient temperature of 22°C.

RESULTS AND DISCUSSION

Water contact angles for all samples (rough and smooth) are listed in Table 2. The advancing and receding angles differ from their values on the smooth surface, even on surfaces with few particles (samples 1 and 2). The vibrated contact angle, however, is affected only when a

TABLE 2 Advancing, θ_A, Receding, θ_R, and Vibrated, θ_V, Contact Angles of Water on Smooth (0) and Increasingly Rough (1–4) Surfaces

Sample	θ_A [deg]	θ_R [deg]	θ_V [deg]	N_P	λ/d
0	125.5	114.4	121.0	0	∞
1	127.9	118.1	121.1	95	10
2	129.5	111.0	120.3	125	7
3	145.5	116.6	126.8	295	3
4	165.2	121.9	132.1	430	2

N_P, average number of particles on the wetting perimeter; λ, average interparticle distance; d, average particle diameter.

threshold roughness is exceeded. The distortion of the contact line due to a single particle can be crudely estimated as $\gamma \times d = 48\,\mu\text{m} \times 73\,\text{mJ/m}^2 \approx 4\,\mu\text{N}$. It therefore appears that even a single particle of that size should be detectable in our setup, hence the variation in the advancing and receding contact angles. Shanahan has given an elegant theoretical description of the deformation of a meniscus caused by local defects [25].

When mechanical energy is provided to the system (*via* acoustic waves) the contact line experiences significant vibrations, and many contortions due to intersecting particles can be avoided. In other words, the external energy input allows the contact line to de-pin from anchoring defects, and the free energy of the system (after cessation of the disturbance) is diminished. At lower particle coverage (samples 1 and 2) the contact line will avoid crossing the rather distant particles. As surface coverage increases this should be less and less probable (samples 3 and 4) and we speculate that, when the distance between adjacent particles, λ, reaches the order of the particle size, contortions cannot be avoided. The vibrated contact angle then becomes dependent on the surface roughness. An estimate of the average interparticle distance is given in the last column of Table 2, in support of our hypothesis.

We now consider only the rougher samples (3 and 4) with respect to the smooth one. The advancing contact angles are shown as a function of the roughness ratio in Figure 3.

The dependence of $\cos\theta_A$ on r is always linear and the slope, $\partial\cos\theta_A/\partial r$, gradually changes from negative to positive as the contact angle on the smooth surface, θ_A^0, decreases. The receding and vibrated [21] contact angles follow a very similar pattern. In other words, θ_A, θ_R, and θ_V all qualitatively agree with Wenzel's prediction. In order to test the Wenzel equation quantitatively, the slopes of the lines

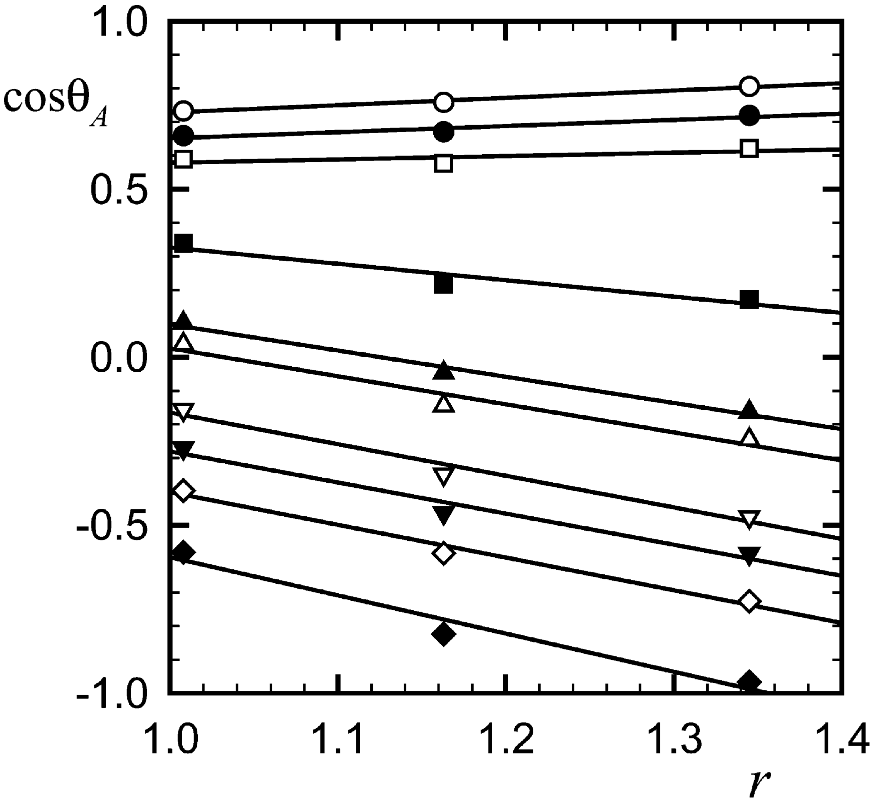

FIGURE 3 Advancing contact angle, θ_V, *versus* Wenzel ratio, *r* (○, hexane; ●, heptane; □, octane; ■, hexadecane; △, dimethylformamide; ▲, methylnaphtalene; ▽, dimethylsulphoxide; ▼, ethylene glycol; ◇, formamide; ◆, water).

shown in Figure 3 are plotted in Figure 4 against the respective angles measured on smooth surfaces.

The solid line represents the Wenzel Equation (8) and, in spite of some scatter, the vibrated contact angles closely follow the theoretical prediction [21]. The fact that θ_V quantitatively obeys the Wenzel equation strongly suggests that θ_V are *de facto* (within the scatter of the measurement) equilibrium contact angles.

The advancing and receding contact angles are more scattered than θ_V (Figure 4), and even the linearity of the dependence can be questioned. Thus, a one-sided consideration could easily lead to the apparent but unjustified conclusion that contact angles measured in a real system do not follow Wenzel's equation. Interestingly, θ_A and θ_R both

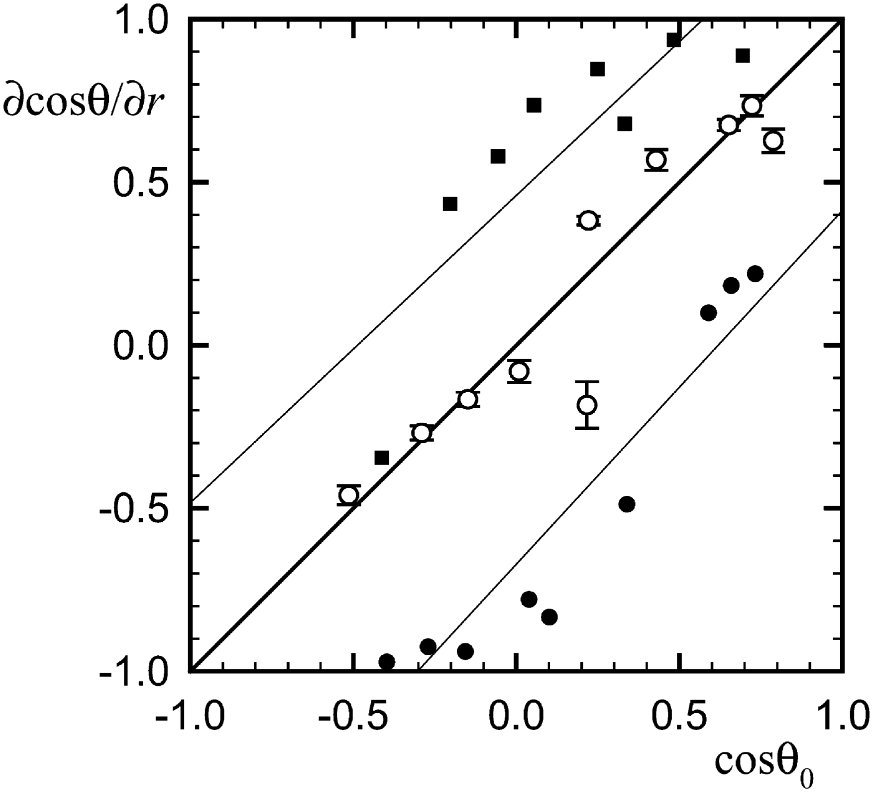

FIGURE 4 Comparison of the experimental Wenzel slope, $\partial\cos\theta/\partial r$, and the theoretical value, $\cos\theta_0$, predicted by the Wenzel equation (solid line): ■, advancing angles; ○, vibrated angles; ●, receding angles.

display, on the average, linear trends parallel to the theoretical Wenzel line and almost equally shifted on both sides of θ_V.

This apparent symmetry, as well as the fact that vibrated contact angles are reported only occasionally [26–28] call for an examination of the average contact angle defined by Equation (11). The vibrated contact angle is compared with the average one in Figure 5.

On the smooth surface the agreement is excellent; on the rough surfaces a discrepancy is seen below about 60° and the rougher the surface the larger the deviation. Similar findings have been reported by Andrieu *et al.* [27] for various substrates, which were both rough and chemically heterogeneous. The two sets of results compare quite favourably (Figure 6).

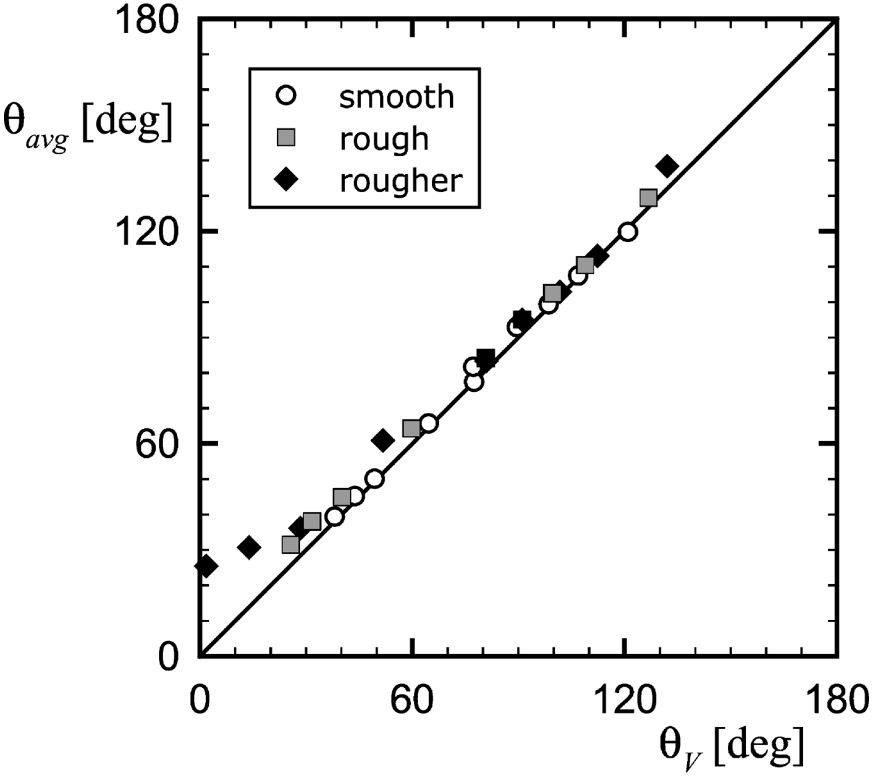

FIGURE 5 Average contact angle, θ_{avg}, *versus* vibrated contact angle, θ_V, on smooth and rough surfaces (○, sample 0; □, sample 3; ◆, sample 4).

The scatter in our data is much smaller, which is understandable given the crude methods of preparation used in Andrieu *et al.* [27]. Thus it appears that the average contact angle can be used instead of the vibrated one as long as the surface is not too rough or the contact angles too small. Whether θ_V underestimates the equilibrium contact angle or θ_{avg} is an overestimate (both for small contact angles) is, at present, not clear.

Perhaps the most useful aspect of contact angles is that they provided a rather easy assessment of the surface energetics. Three perfluorinated, strongly hydrophobic surfaces—Teflon AF1600 (this study), FC722 [29], and FEP [17]—are compared in Figure 7, where the adhesion tension is plotted as a function of the surface tension of the liquid.

It can be seen that the trends are very similar. Results for FEP follow the same dependence, though scatter varies largely between

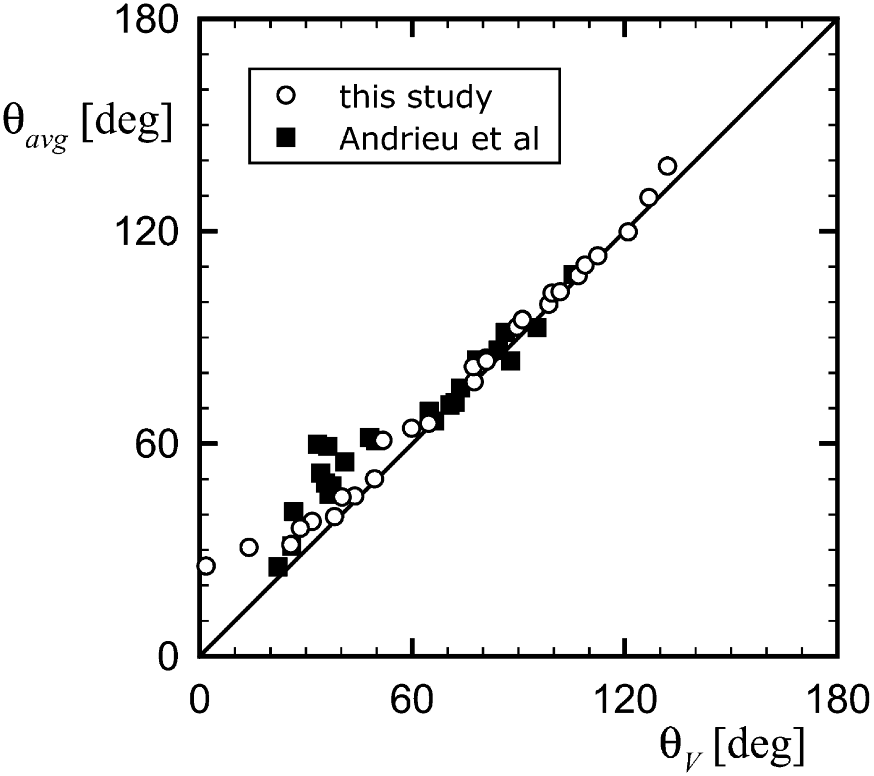

FIGURE 6 Average contact angle, θ_{avg}, *versus* vibrated contact angle, θ_V, on various surfaces (○, all data points from Fig. 5; ■, Andrieu *et al.* [27]).

different laboratories. The commercially available coatings FC722 and AF1600 are significantly more hydrophobic. In Figure 7 we have used the $\gamma\cos\theta$ *versus* γ format recommended by Neumann and coworkers [3, 29]. The dependences are quite nicely fit with second-order polynomials, and therefore we revert to the classic Zisman format (cos θ *versus* γ), which has the advantages of being linear (at least partly) and making the extrapolation to zero contact angle very illustrative.

A Zisman plot of the vibrated contact angles on a smooth AF1600 surface is shown in Figure 8. The first four points are well described by the Zisman Equation (2).

All other points deviate positively from the linear trend. The concavity of the Zisman plot at higher values of the liquid surface tension is predicted by both theories. The equation-of-state approach,

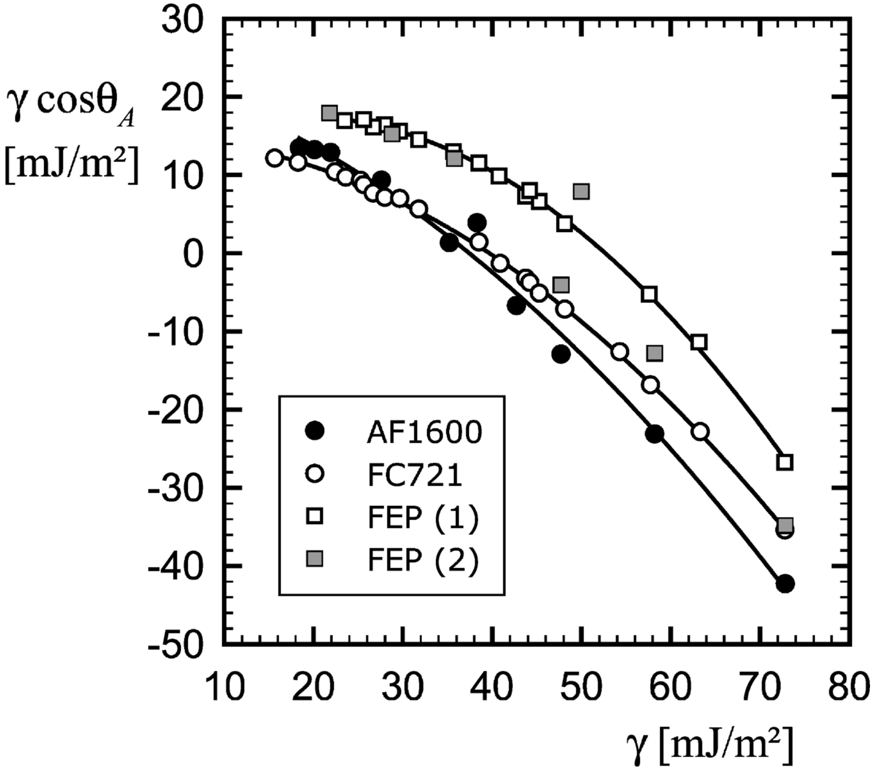

FIGURE 7 Wetting tension, γ cos θ, *versus* liquid surface tension, γ, for several fluropolymer surfaces: ●, Teflon AF1600 (this study); ○, FC722 [29]; □, FEP [29]; ■, FEP [17].

Equation (3), can be expanded as

$$\cos\theta = 1 - \frac{1}{\gamma_S}(\gamma - \gamma_S) + \left(\frac{3}{4\gamma_S^2} - 2\beta\right)(\gamma - \gamma_S)^2 + O[(\gamma - \gamma_S)^3]. \tag{12}$$

Using the value $\beta = 124.7\,\mathrm{m^2/N^2}$ [7], it is estimated that the quadratic term will be positive for any surface with $\gamma_S < 55\,\mathrm{mJ/m^2}$. Similarly, Equation (5) can be expanded as [12]

$$\cos\theta = 1 - \frac{1}{\gamma_S}(\gamma - \gamma_S) + \frac{3}{4\gamma_S^2}(\gamma - \gamma_S)^2 + O[(\gamma - \gamma_S)^3], \tag{13}$$

and it is easily seen that the second-order term is always positive. However, both expressions fail to predict the experimentally observed curvature of the plot in Figure 8.

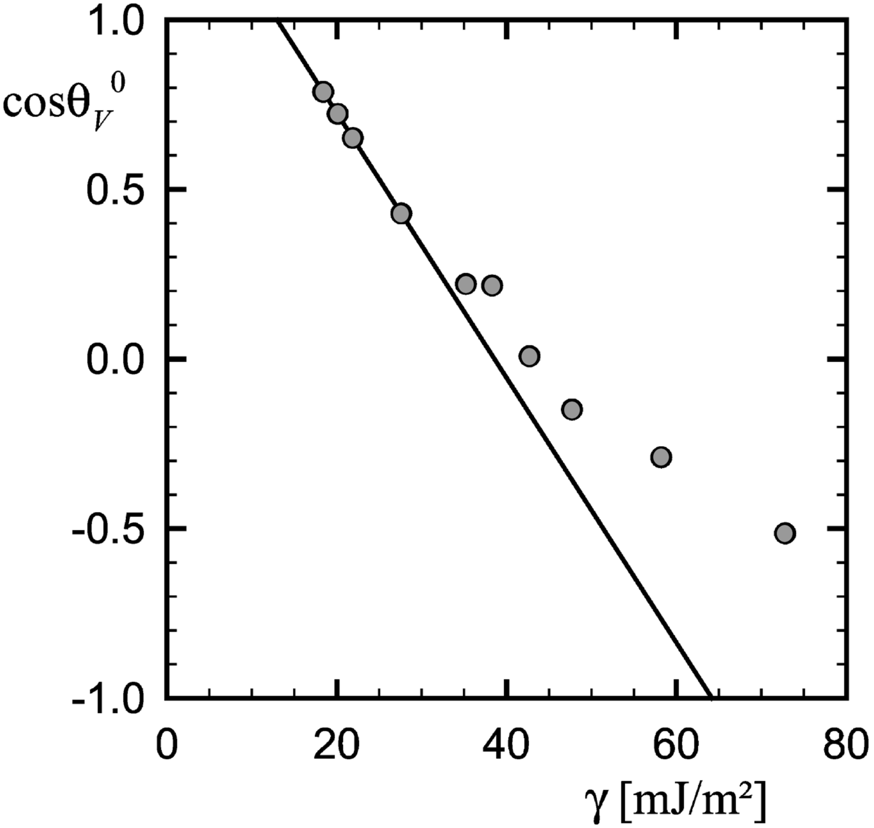

FIGURE 8 Zisman Plot of the cosine of the vibrated contact angle, θ_V, on smooth Teflon AF1600 surface *versus* the liquid surface tension, γ. The solid line is the best fit through the data points for alkanes (hexane, heptane, octane, and hexadecane).

The four points described by the Zisman Equation in Figure 8 are obtained with various alkanes and all other liquids deviate from the straight line. It is, therefore, plausible that the "alkane line" can be used to determine the LW component of the surface tension for any liquid used. An estimate of the AB component can then be obtained through Equation (4). The difference between the total surface tension and the surface tension corresponding to the alkane line is compared with the literature values of the AB component [4] in Figure 9.

The overall agreement is fairly good (especially with regard to the notorious inaccuracy of the γ^{AB} values) and supports the above

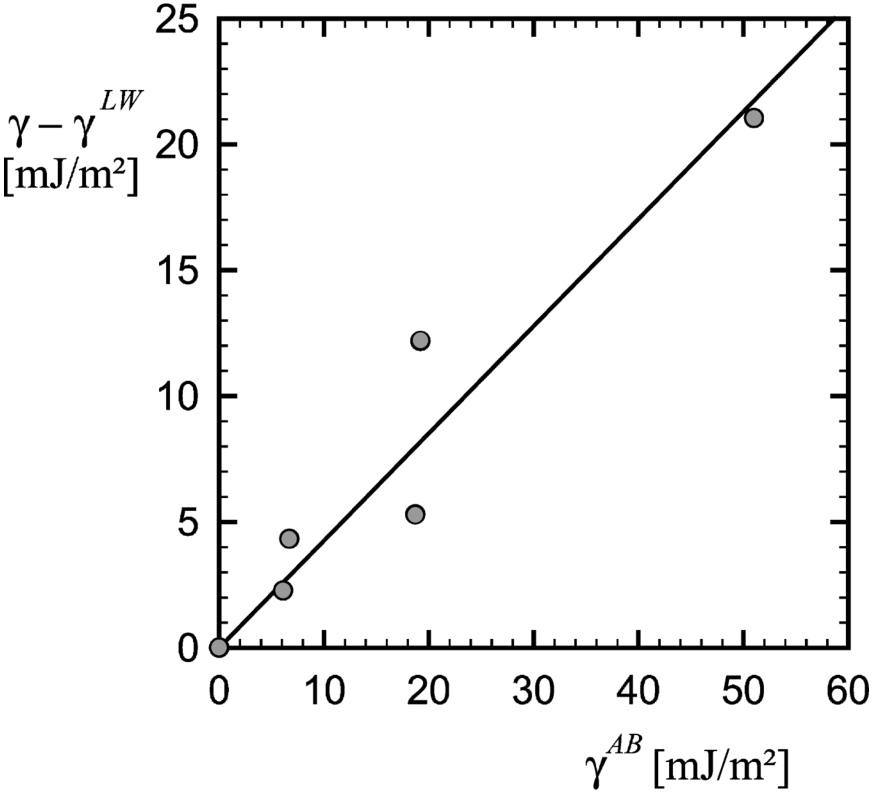

FIGURE 9 Comparison between the difference ($\gamma - \gamma^{LW}$) and literature values [4] for γ^{AB}. The slope of the line going through the origin is 0.43. γ^{LW} is estimated from the data shown in Figure 8 as the liquid surface tension required for the angle made by any liquid to fall exactly on the alkane line.

interpretation. Quantitatively, however, the slope in Figure 9 is only about 43% of the expected value for reasons that are not clear.

The Zisman approach, as described, can be applied to the rough surfaces under investigation, and the outcome is presented in Figures 10 and 11 as well as in Table 3. Figure 10 shows that the critical surface tension of wetting increases as the Wenzel ratio increases. The trend is the same for all three types of contact angles, but the vibrated contact angles are closer to the receding ones.

The critical surface tension of wetting for smooth AF1600 is $13\,\mathrm{mJ/m^2}$ (see Table 3). This is slightly higher than typical values obtained from advancing contact angles. Depending on the care taken during sample preparation, we have recorded values in between 12

TABLE 3 Zisman's Critical Surface Tension of Wetting Obtained from Different Types of Contact Angles on Smooth and Rough AF1600 Surfaces

Type of Angle	Smooth	Rough 3	Rough 4
Vibrated	13.0 (2)	16.5 (3)	18.9 (4)
Advancing	12.2 (2)	14.5 (3)	16.0 (5)
Receding	13.2 (2)	17.0 (2)	19.8 (10)

Standard errors are given in parentheses.

and $13\,\mathrm{mJ/m^2}$ (a more detailed discussion of the critical surface tension of wetting of Teflon AF with respect to composition can be found in Quinn *et al.* [30]).

The fact that vibrated contact angles, which supposedly are a good approximation of the equilibrium ones, give a rather different result

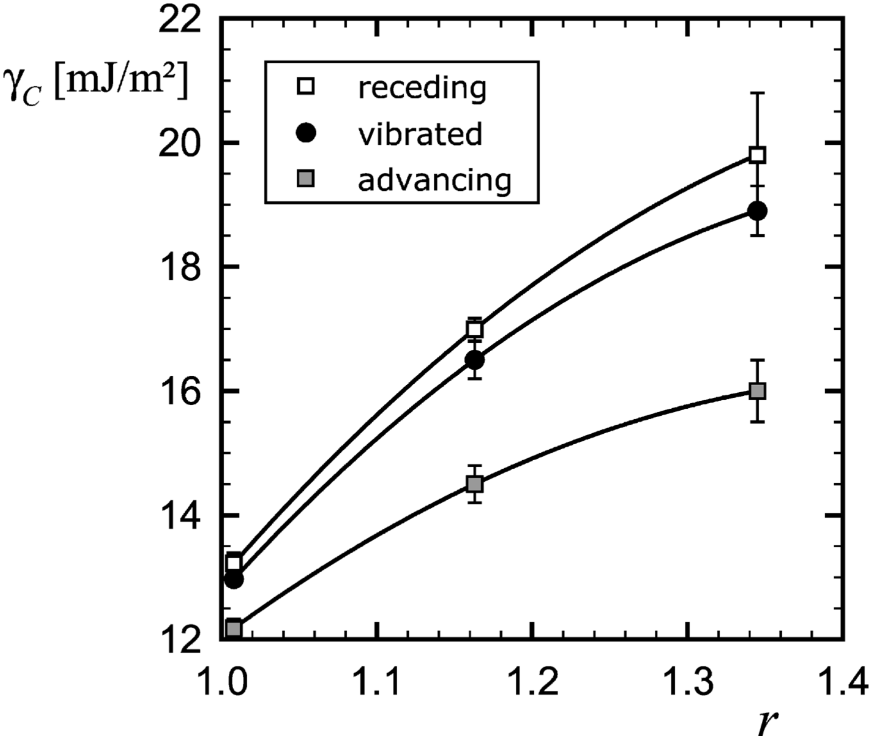

FIGURE 10 Variation of the critical surface tension of wetting, γ_C, with Wenzel ratio, r: □, receding; ●, vibrated; ■, advancing contact angles.

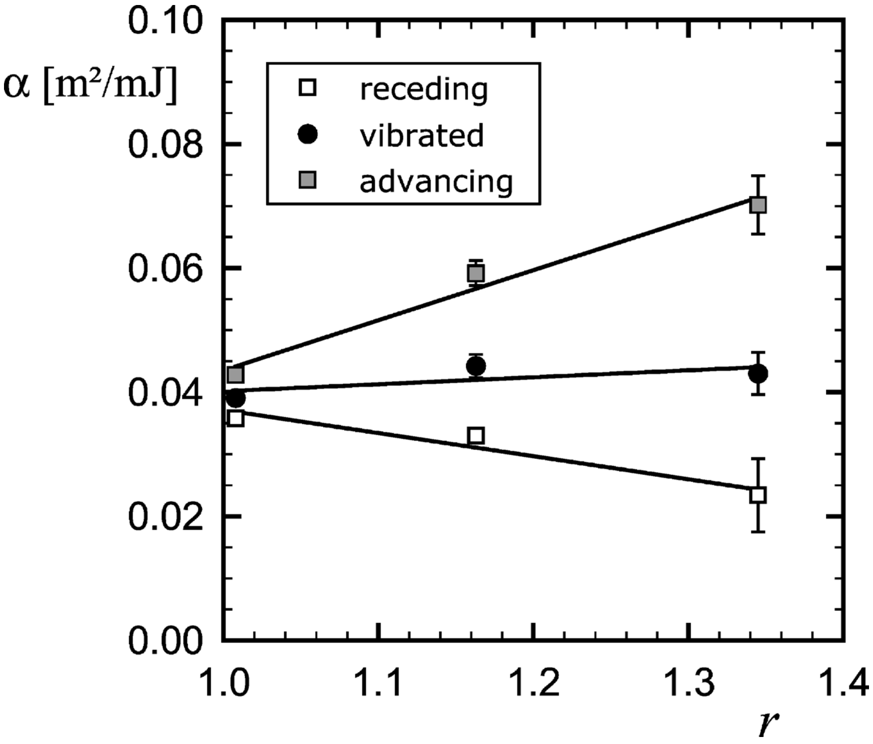

FIGURE 11 Variation of Zisman's slope, α, with Wenzel ratio, r: □, receding; ●, vibrated; ■, advancing contact angles.

in comparison with advancing angles runs somewhat contrary to the widely adopted opinion that advancing contact angles are most representative of the polymer surface [1, 3, 5, 12]. It is conceivable that the advancing angles yield a more consistent value characteristic of the main low-energy component (the exposed chemical groups of the pure polymer) in spite of imperfections present on the surface, while the vibrated contact angles correspond to the properly weighted average wettability of the surface in question, including the importance of the surface defects.

Little attention is usually paid to the Zisman slope α (shown in Figure 11). According to Equations (12) and (13) it should represent the reciprocal of the critical surface tension of wetting, but values obtained in this way are very different [12]. Differences are so significant that meticulous authors will actually report two values for the same set of results (Drummond *et al.* [31] is an example concerning

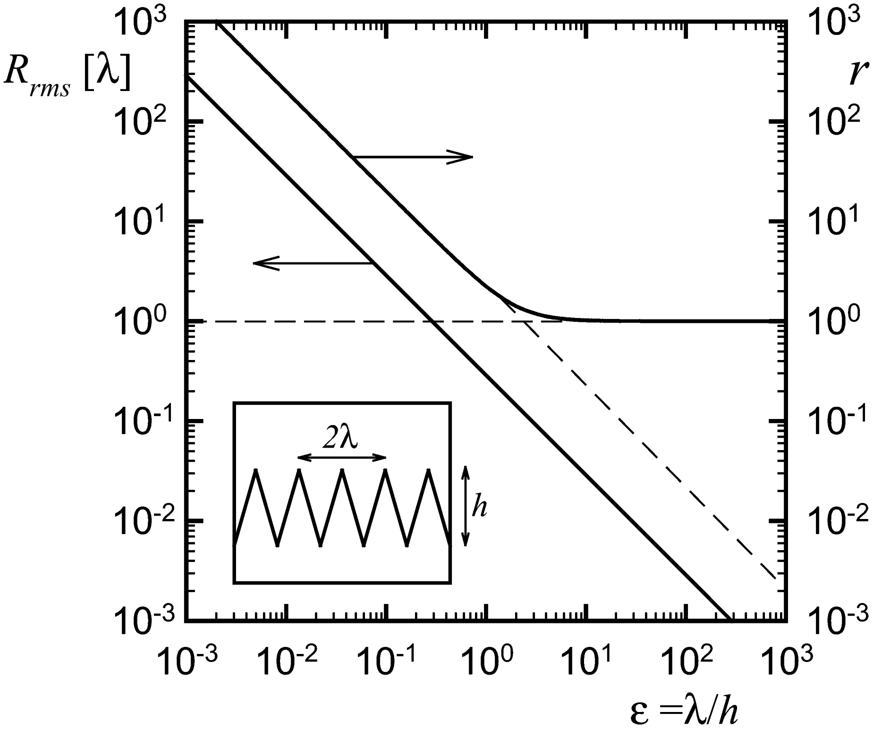

FIGURE 12 Comparison of RMS roughness, R_{rms}, and Wenzel ratio, r, as functions of the aspect ratio, ε $(= \lambda/h)$, for a triangular wave (λ is the wavelength and h is the amplitude; see inset).

Teflon AF1600 and AF2400). Therefore, we consider the slope α as an independent parameter. As can be seen in Figure 11, it is positive for θ_A, negative for θ_R, and practically nonexistent for θ_V. The symmetry between advancing and receding contact angle behaviour is again evident.

The changes observed in Figures 10 and 11 can be accounted for by combining the Wenzel and Zisman equations. If Equation (2) for the rough surface is written as

$$\cos\tilde{\theta} = 1 - \tilde{\alpha}(\gamma - \tilde{\gamma}_C), \tag{14}$$

it then follows that [32]

$$\begin{aligned} \tilde{\alpha} &= r\alpha \\ \tilde{\gamma}_C &= \gamma_C + \frac{1}{\alpha}\left(1 - \frac{1}{r}\right). \end{aligned} \tag{15}$$

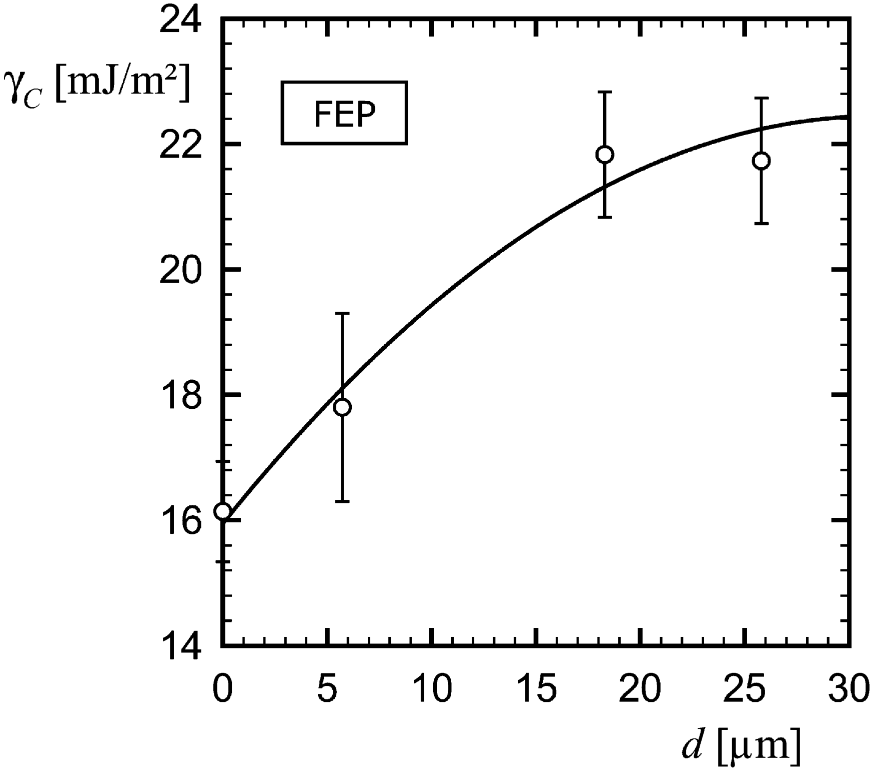

FIGURE 13 Variation of the critical surface tension of wetting, γ_C, with grit size, d: Data for FEP from Good *et al.* [17].

Equation (15) explains the dependences shown in Figures 10 and 11, but only qualitatively. The relation between the slope α and the extrapolated value γ_C is more intricate than predicted by Equations (12) and (13).

Finally, we re-examine the data of Good *et al.* [17] in order to compare our findings with results from an independent source. Unfortunately, the roughness ratio was not reported in Good *et al.* [17]. Since the samples were abraded with different grades of sandpaper, we suppose the rms roughness, R_{rms}, is proportional to the dimension of the grain (grit size), d. The relation between R_{rms} and r is strongly influenced by the aspect ratio of the defect, $\varepsilon = \lambda/d$. As an illustration the rms roughness and the roughness ratio for a triangular wave are plotted in Figure 12.

Since the rough surfaces in Good *et al.* [17] were extensively ground, we can assume that the aspect ratio was small, which in turn

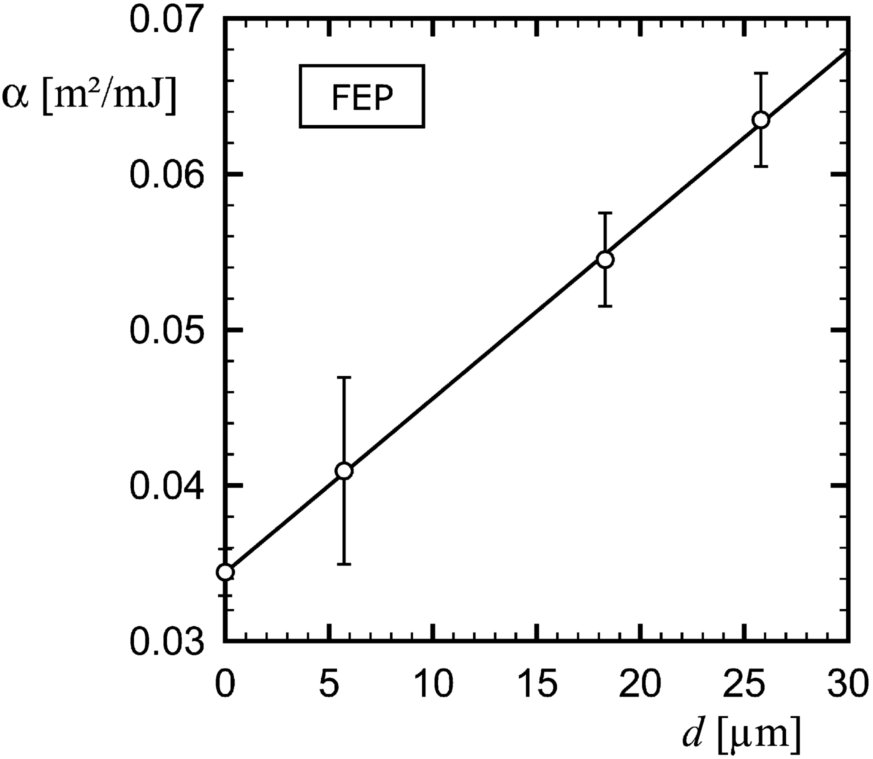

FIGURE 14 Variation of Zisman's slope, α, with grit size, d: Data for FEP from Good *et al.* [17].

implies the proportionality $r \sim d$. Therefore, in the subsequent analysis we have used d instead of r.

The Zisman plots for the smooth and rough FEP studied by Good *et al.* [17] are very similar to our result, shown in Figure 8. A deviation from the linear trend is always present and always positive. The variations in the critical surface tension and the slope are shown in Figures 13 and 14.

Essentially we recover the behaviour already shown in Figures 9 and 10 and qualitatively accounted for by Equations (15). Thus, treating a set of independent results we reach the same conclusions as deduced from our own measurements, in strong support of our claims.

CONCLUSION

Reproducible advancing and receding contact angles have been measured on Teflon AF1600-coated surfaces (rough and smooth). By subjecting the three-phase system to acoustic vibrations, the contact angle hysteresis has been effectively eliminated. The vibrated contact angles follow the trend predicted by the Wenzel equation and therefore are the closest available approximation for equilibrium contact angles. Provided that the surface is not too rough/heterogeneous, or the angles too small, the average contact angle is also a plausible approximation.

The wettability of a fluoropolymer surface can be conveniently represented in terms of a Zisman plot. The alkanes give a straight line, which can be extrapolated to obtain the value of the critical surface tension of wetting. Liquids whose surface tension arises from more than purely dispersive interactions deviate from the linear dependence in a manner described (at least qualitatively) by various contact angle theories.

The critical surface tension of wetting of the solid surface depends on the type of contact angles used in the analysis. The advancing contact angles are widely accepted to be characteristic of the major component (*i.e.*, the characteristic chemical groups of the polymer) on the surface. The vibrated contact angles appear to be more representative of the average wettability of the sample, *i.e.*, including the presence of defects. The critical surface tension increases with roughness in agreement with the Wenzel equation. The physical explanation is rather simple—the interfacial area is r times as large as the nominal area considered.

The wettability of rough surfaces can be assessed with traditional measurement techniques and can be accounted for within the existing theoretical framework.

REFERENCES

[1] Adamson, A. W. and Gast, A. P., *Physical Chemistry of Surfaces*, 6th ed. (Wiley, New York, 1997).

[2] Berg, J. C., *Wettability* (Marcel Dekker, New York, 1993).

[3] Neumann, A. W. and Spelt, J. K., *Applied Surface Thermodynamics* (Marcel Dekker, New York, 1996).

[4] van Oss, C. J., *Interfacial Forces in Aqueous Media* (Marcel Dekker, New York, 1994).

[5] Zisman, W. A., *Adv. Chem. Ser.* **43**, 1–51 (1964).

[6] Blake, T. D., In: *Surfactants*, Tadros, T. F., Ed. (Academic Press, London, 1984), Chap. 10.

[7] Li, D. and Neumann, A. W., *J. Colloid Interface Sci.* **137**, 304–307 (1990).

[8] Fowkes, F. M., Attractive forces at interfaces, In: *Chemistry and Physics of Interfaces*, Ross, S., Ed. (ACS, Washington, D.C., 1965), pp. 1–12.

[9] Good, R. J. and van Oss, C. J., In: *Modern Approaches to Wettability*, Schrader, M. E., and Loeb, G. I., Eds. (Plenum Press, New York, 1992), pp. 1–27.

[10] Good, R. J., *J. Adhesion Sci. Technol.* **6**, 1269–1302 (1992).

[11] van Oss, C. J., Chaudhury, M. K., and Good, R. J., *Chem. Rev.* **88**, 927–941 (1988).

[12] Good, R. J., *J. Colloid Interface Sci.* **59**, 398–419 (1977).

[13] Everett, D. H., *Pure Appl. Chem.* **52**, 1279–1293 (1980).

[14] Good, R. J., *J. Am. Chem. Soc.* **74**, 5041–5042 (1952).

[15] Adam, N. K. and Jessop, G., *J. Chem. Soc.* **127**, 1863–1868 (1925).

[16] Kwok, D. Y. and Neumann, A. W., *J. Phys. Chem. B* **104**, 741–746 (2000).

[17] Good, R. J., Chaudhury, M. K., and Yeung, C., In: *Mittal Festschrift on Adhesion Science and Technology*, van Ooij, W. J., and Anderson, J., Eds. (VSP, Utrecht, 1998), pp. 181–197.

[18] Neumann, A. W., Renzow, D., Reumuth, H., and Richter, I. E., *Fortschr. Kolloide Polymere* **55**, 49–54 (1971).

[19] Mason, S. G., *Wetting and Spreading—Some Effects of Surface Roughness*, In: *Wetting, Spreading and Adhesion*, Padday, J. F., Ed. (Academic Press, London, 1978), pp. 321–386.

[20] DuPont, *Product Information Sheet* **Teflon AF**, Cat. No., DuPont, Wilmington, DE, H-44015–44013 (1998).

[21] Fabretto, M., Sedev, R., and Ralston, J., In: *Contact Angle, Wettability and Adhesion*, Mittal, K. L., Ed. (VSP, Utrecht, 2003), pp. 161–173.

[22] Hayes, R. and Ralston, J., *Colloids Surf. A* **93**, 15–23 (1994).

[23] Hayes, R. and Ralston, J., *J. Colloid Interface Sci.* **159**, 429–438 (1993).

[24] Hayes, R. and Ralston, J., *Colloids Surf. A* **80**, 137–146 (1993).

[25] Shanahan, M. E. R., *J. Phys. D. Appl. Phys.* **22**, 1128–1135 (1989).

[26] Della Volpe, C., Maniglio, D., Siboni, S., and Morra, M., *Oil Gas Sci. Technol.* **56**, 9–22 (2001).

[27] Andrieu, C., Sykes, C., and Brochard, F., *Langmuir* **10**, 2077–2080 (1994).

[28] Decker, E. L. and Garoff, S., *Langmuir* **12**, 2100–2110 (1996).

[29] Kwok, D. Y. and Neumann, A. W., *Adv. Colloid Interface Sci.* **81**, 167–249 (1999).

[30] Quinn, A., Sedev, R., and Ralston, J., *J. Phys. Chem. B* **107**, 1163–1169 (2003).

[31] Drummond, C. J., Georgaklis, G., and Chan, D. Y. C., *Langmuir* **12**, 2617–2621 (1996).

[32] Chow, T. S., *J. Phys.: Condens. Matter* **10**, L445–L451 (1998).